Multi-Wavelength Optical Fiber Refractive Index Profiling by Spatially Resolved Fourier Transform Spectroscopy

Andrew D. Yablon, *Member, IEEE*

***Abstract*—A non-destructive technique to measure an optical fiber's refractive index profile with sub-μm spatial resolution over a wavelength range spanning more than one octave (from 480 to 1040 nm) in a single measurement is described. Data showing the variation of refractive index with wavelength for several fiber types is presented.**

***Index Terms*—Optical fibers, Optical fiber measurements, Fourier spectroscopy.**

I. Introduction

CRITICAL fiber performance metrics, including dispersion, modal effective area, or grating spectra, are more accurately predicted with knowledge of the spectral dependence of the fiber's refractive index profile. Since most practical optical fibers are doped with a complex and proprietary mix of multiple species that may contribute to the refractive index in a non-additive way, an *in situ* method for analyzing the spectral dependence of a fiber of arbitrary composition is desirable. All previous optical fiber refractive index profiling methods [1-9] provide data at only one single probe wavelength, which is typically far outside the operating band of the fiber. Therefore, the spectral dependence of the fiber's refractive index profile can only be obtained from these methods by repeating the measurement at numerous discrete wavelengths [9]. Partly for this reason, the spectral dependence of the refractive index has only been characterized for select dopants at particular concentrations [9-13]. Furthermore, these studies either required wafer-thin fiber slices [9], which are inherently destructive, expensive to prepare, and permit stress relaxation, or they were performed on homogeneous bulk samples [10-12] or samples extracted from fiber performs [13], which are poor substitutes for actual fiber samples since they have different thermal histories, minimal dopant diffusion, and have not experienced fiber draw. This paper describes a new, non-destructive, *in situ* technique for obtaining spectrally resolved refractive index profiles for arbitrary optical fibers across an entire octave with sub-μm spatial resolution in a single measurement. Our technique can be understood as a spatially resolved extension of Dispersive Fourier Transform Spectroscopy (DFTS) [14] and it therefore enjoys the same signal-to-noise-ratio advantage (the so-called *Multiplex* or *Fellget Advantage*) because the brightness of a broadband probe signal scales with the bandwidth while the detector noise does not [15].

Manuscript received May 14, 2009; revised August 19, 2009.

A.D. Yablon is with Interfiber Analysis, Livingston, NJ 07039 USA (phone: 973-992-5148; fax: 973-488-7134; e-mail: andrew_yablon@interfiberanalysis.com).

II. Experimental Setup

A. Instrumentation

A schematic of the experimental setup appears in Fig. 1 and is a modification of the Transverse Interferometric Method (TIM) in which a fiber is placed in the sample arm of a Mach-Zehnder interference microscope [1,3-7,9]. The Michelson architecture employed by almost all Fourier transform spectrometers [14,15] has been shown to be less suitable for optical fiber measurements compared to the Mach-Zehnder configuration because substantial aberrations are incurred by double traversal of the fiber sample [1]. No cleave is necessary since the probe light travels transversely across the optical fiber [5-7], therefore the fiber could even carry a signal during the index measurement. Since the polymer buffer surrounding most optical fibers is turbid, it must be removed in the vicinity of the index measurement, although in principle it can be restored after the measurement using fiber recoat technology. The fiber was inserted into refractive index matching oil and imaged by a high-NA (up to 1.4) oil-immersion objective lens that permitted sub-μm spatial resolution. For the experiments described here, a Leitz interference microscope [1,5-7,9,15,16] was employed, although an equivalent interferometer can be constructed from conventional optical components [3,4]. A tungsten-halogen lamp with a visible-light blocking filter was combined with an identical unfiltered lamp to yield a high-brightness spatially incoherent wideband optical source, which avoided coherent noise effects that otherwise plague spatially resolved interferometry [6,18].

Traditionally, TIM required the interferometer to superpose

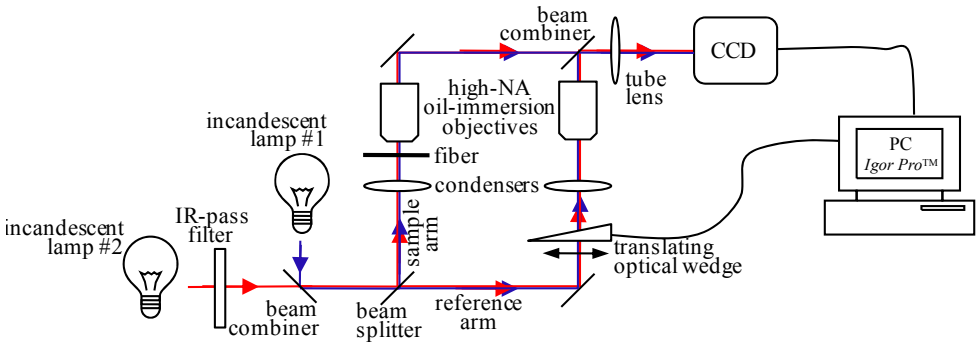

Fig. 1. Schematic illustration of experimental setup [26]

a number of bright and dark interference fringes across amagnified image of the fiber, and the spatial deflection of these fringes would be detected and converted into a refractive index profile [1,3,5-7,9]. In contrast, the present method uses an optical wedge phase shifter [19] to uniformly shift the optical path length of the reference arm, thereby generating a distinct interferogram for each spatial position (pixel) in the image as a function of applied phase shift. General advantages of *phase-shifting* (or *phase-stepping*) *interferometry* (PSI) [4,19,20] over spatial fringe detection include: (1) robustness to fringe spacing or orientation; (2) insensitivity to illumination inhomogeneities; and (3) the opportunity to expand the field of view by stitching multiple frames together.

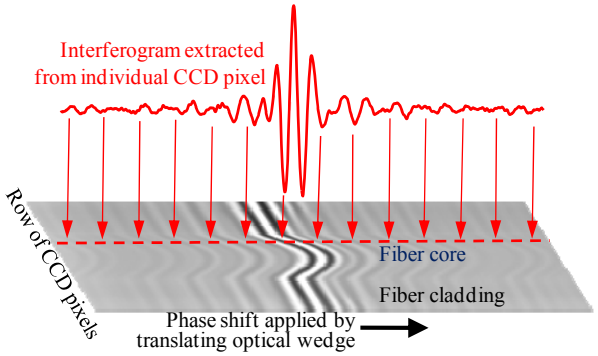

Fig. 2. Sample interferograms acquired for a graded index multimode (GI-MMF) optical fiber. [26]

The detector was an analog monochrome 8-bit 640-by-480-pixel silicon CCD (Hitachi KP160) with excellent visible and near-IR responsivity. During a 68-second-long data acquisition scan, 2048 individual CCD frames were acquired at video rate (30 frames per second) while the continuously translating optical wedge imposed a total phase shift of about 18 μm of optical path. Data processing on a desktop PC required about 3 minutes. Both acquisition and processing were accomplished by software written in the Igor Pro™ [21] environment.

B. Processing Algorithm

Fig. 2 shows a sample interferogram obtained from a commercial (*Fiber Instrument Sales*, Oriskany, NY) 125 μm diameter graded-index multimode fiber (GI-MMF). The fast-Fourier-transform (FFT) was applied separately to each pixel location as a function of applied phase shift. Each spatial frequency in the resulting FFTs corresponded to a probe wavelength and a plot of the FFT amplitudes (Fig. 3) reveals the optical power spectrum detected by the CCD.

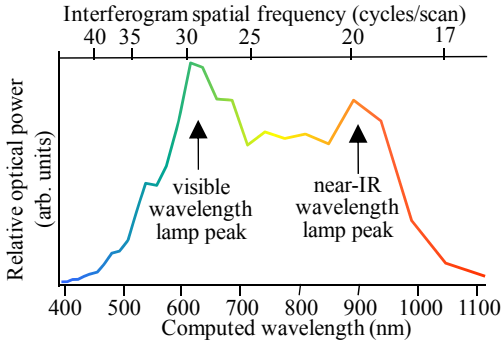

Fig. 3. Amplitude spectrum obtained from fast Fourier transform of interferogram depicted in Fig. 2. The refractive index is determined from only the phase components of the Fourier transforms. [26]

In separate experiments, the relationship between the optical probe wavelength and the spatial frequency of the FFT was calibrated with the aid of several narrow-linewidth bandpass filters. The peak FFT amplitude peaks was measured when the interferometer was exclusively illuminated by filtered light with central wavelengths of 436 nm (full-width half-maximum, FWHM of 25 nm), 530 nm (FWHM of 1 nm), 546 nm (FWHM of 35 nm), 589 nm (FWHM of 10 nm), 632 nm (FWHM of 10 nm), or 700 nm (FWHM of 33 nm). The relationship between the spectral peak and the interferogram spatial frequency was found to be substantially linear. Based on this calibration, the uncertainty of the probe wavelength associated with a interferogram spatial frequency is estimated to be about ±0.5%. Since the measured refractive index scales linearly with the wavelength, the associated fractional error in Δn is the same magnitude, which corresponds to less than $\pm 1 \times 10^{-4}$ for most practical fiber refractive index profiles.

At each optical probe wavelength, the relative phase of the FFT between the various pixels in the image reveals the optical path length variation as a function of spatial position in the image, modulo 2π. Phase ambiguities were robustly resolved using Goldstein's 2-dimensional phase unwrapping algorithms [19-21]. Unwrapped phase images obtained from the GI-MMF fiber for several optical probe wavelengths are

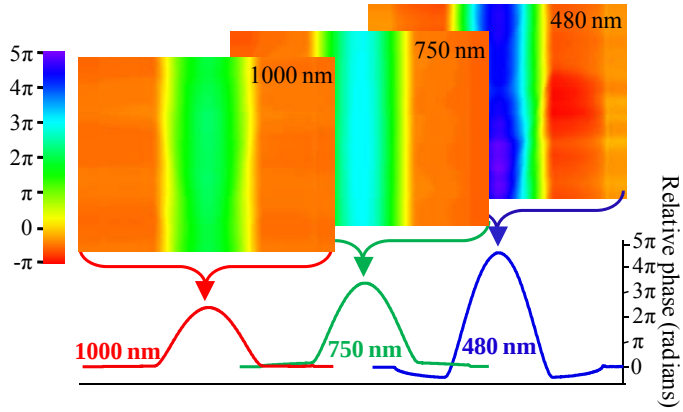

Fig. 4. False color representations of the (unwrapped) phase spatial distribution measured for the same graded-index multimode fiber (GI-MMF) depicted in Figure 2 at several representative optical wavelengths. The false color depicts relative phase in radians as shown in the colorscale at left.

shown in Fig. 4. The unwrapped phase as a function of transverse position was obtained by averaging the phase images along the axial direction as demonstrated in Fig. 4.

The unwrapped phase was converted into a refractive index profile at each particular optical probe wavelength using one of two methods. Axisymmetric fibers permitted the application of the inverse Abel transform [1-3,8,22,23]. Non-axisymmetric fibers, such as Polarization Maintaining (PM) fibers, were processed using a tomographic reconstruction algorithm [2,6,7,21,22] over a 180 degree range of azimuthal fiber rotation angles.

III. Results

It is convenient to express the measurement results in terms of a relative refractive index, termed $\Delta n(\lambda)$, where

$$\Delta n(\lambda) = n(\lambda) - n_{\text{silica}}(\lambda), \tag{1}$$

n is the measured refractive index, n_{silica} is the refractive index of the silica cladding, and λ is wavelength.

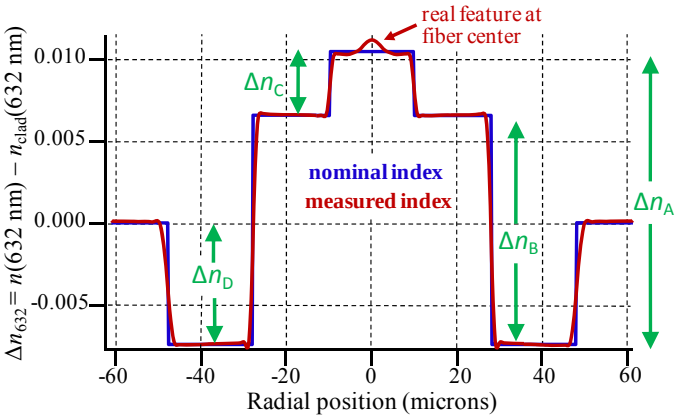

Fig. 5. Comparison between nominal data for the NPL reference fiber [23] and measured data at 632 nm. The feature at the center of the measured data is real but is not included in the refractive index specification. The gentle tilt observed in some of the regions is consistent with Fig. 7(b) of reference [8].

Figure 5 compares the refractive index of an industry standard multistep reference fiber [8,23] with measured data at 632 nm. This reference fiber is specified in terms of the refractive index difference between various regions as detailed in Table 1. The largest discrepancy between the measurement and the reference fiber is observed for Δn_C since, as noted by Marcuse [1], the noise of refractive index profile obtained by transverse interferometery is largest at the very center of the fiber because noise is accumulated by the inversion algorithm (Abel integral or tomography) as it steps in from the outside. A similar argument states that fiber regions with a small cross sectional area (such as the core of single-mode fibers) suffer from elevated noise because there is less total signal available from these regions compared to regions with large cross sectional area (such as a fiber's cladding). Based on these results, we may state that the accuracy of the technique achieved here is on the order of 1×10^{-4} (in units of refractive index). It is noteworthy that unlike commercial refracted near field (RNF) measurements, which are inherently amplitude measurements, the present technique is a phase measurement, and therefore it does not require calibration against the reference fiber shown in Fig. 5 nor does it suffer from measurement drift.

TABLE I
Comparison between Reference Fiber and Measured Data

Region	Nominal value	Measured value	Discrepancy
Δn_A	0.01785	0.01773	1.2×10^{-4}
Δn_B	0.01395	0.01399	-4.0×10^{-5}
Δn_C	0.00390	0.00372	1.8×10^{-4}
Δn_D	0.00740	0.00749	-9.0×10^{-5}

The index differences between regions listed in the left column [23] correspond to the differences indicated by vertical green arrows in Figure 5.

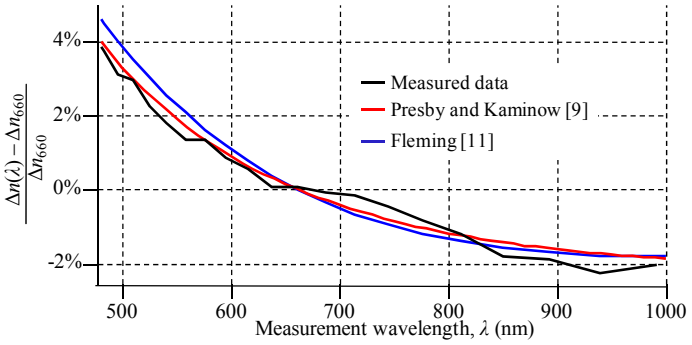

Fig. 6. Comparison between measured normalized refractive index for core center of the graded-index multimode fiber shown in Figures 2 and 4 (GI-MMF) with values computed from [9] and [11]. The discrepancy with the measured data is attributed to noise in the measurement.

Figure 6 compares the variation of measured refractive index versus wavelength for the core region of the Graded-index multimode fiber (GI-MMF) depicted in Figs. 2 and 4 with curves generated from the fitting parameters recommended in [9] and [11]. The data in Fig. 6 are normalized with respect to $\Delta n_{660}=\Delta n(660\text{ nm})$ since the wavelength used by most commercial fiber and preform profilers is at, or near, 660 nm. Therefore this plot provides an estimate as to the error in Δn incurred by ignoring its spectral dependence. Aside from noise fluctuations, the measured results in Figure 6 are seen to agree very well with the previous publications.

The spectral dependence of the refractive index profile measured on standard single-mode fiber (*Corning SMF-28*) is compared to that of a photosensitive fiber (*Thorlabs*, Inc.) in Fig. 7. The spectral dependence of the photosensitive fiber's core is clearly much larger than standard SMF. The spectral dependence of the SMF-28 index profile shown in Fig. 7 provides a quantitative explanation for the discrepancy between the traces appearing in Fig. 10(b) of reference [8], which were acquired at different wavelengths. Although the precise composition of these fibers is known only to their manufacturers, strong spectral dependence may result from dopants intended to promote photosensitivity. Note that the spatial resolution at each wavelength is more than adequate to robustly resolve the fiber's strong *central dip* or *burnoff* region. Fig. 7 also demonstrates that although the spatial resolution is indeed sub-µm, it deteriorates at longer wavelengths, which is a fundamental optical limitation.

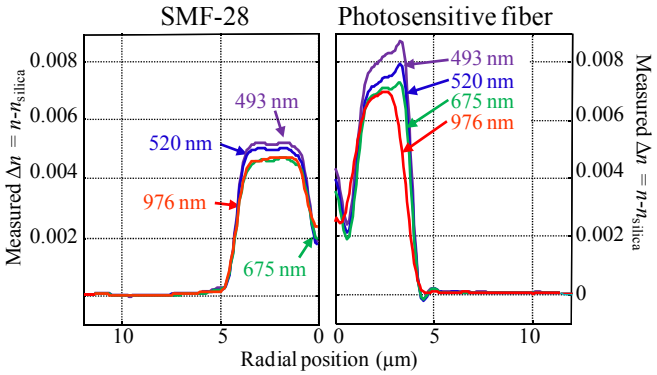

Fig. 7. Refractive index profile spectral dependence for *Corning SMF-28* (*left*) and a commercially available photosensitive fiber (*right*). Only one half of each fiber is shown to permit a more direct comparison of the index profile's spectral dependence. The profiles at longer wavelengths have a smaller Δn, which is typical for most fibers. The spectral dependence of the refractive index profile in the photosensitive fiber is clearly larger than in the *SMF-28*. The sub-µm spatial resolution of the technique is demonstrated by the precise resolution of the "center dip" or "burn-off" region in both fibers at all wavelengths. The raised region at the very center of the photosensitive fiber's center-dip is a real feature and not a measurement artifact. Slightly inferior spatial resolution is evident at the longer wavelengths, which is a fundamental optical limitation.

Figure 8 shows the variation of normalized refractive index versus wavelength for regions of interest in several commercially available (from *Newport Corp.*, *Thorlabs Inc.*, and *Fiber Instrument Sales*) fibers. The normalization with respect to Δn_{660} (listed in the legend for each fiber) permits a diversity of fiber compositions to be presented together on a single plot. Not surprisingly, the core of the high-NA fiber shows enormous spectral dependence whereas spectral dependence of the 0.22 NA fluorine-doped cladding is surprisingly flat. The stress rod was measured in a "Panda" style PM fiber and was presumably boron-doped. To the best of our knowledge, the spectral dependence of Δn for Er-doped and Yb-doped fibers are shown for the first time in Fig. 8 and it is noteworthy that the data extends to the operating band of the Yb-doped fiber and a pump absorption band of the Er-doped fiber. Following [9], the material dispersion can be determined from the data in Fig. 8 by curve fitting followed by differentiation.

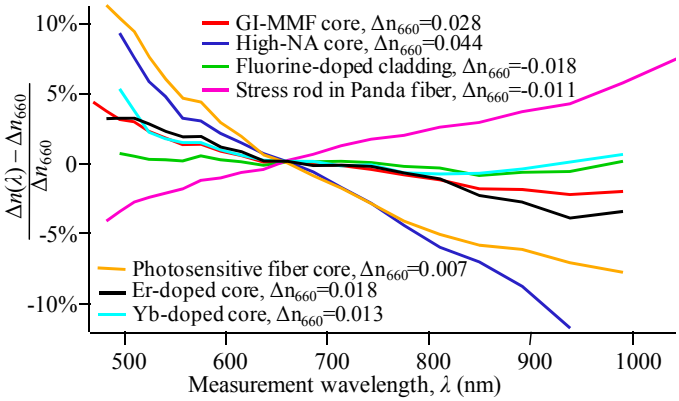

Fig. 8. Refractive index normalized to value at 660 nm for several representative silica fiber compositions. Note that the vertical axis, which indicates the %-error incurred by ignoring the index profile's spectral dependence, corrects a typo appearing in [26]. The spectral dependence of the photosensitive fiber (*mustard line*) shown in Fig. 7 is evidently much larger than the core of the graded-index multimode fiber (*orange line*).

IV. Discussion and Future Directions

Instrumentation improvements could extend the capabilities demonstrated here. For example, the spectral bandwidth of these measurements was constrained by the bandwidths of the lamps and CCD as well as by the degree of chromatic correction in the imaging optics. Specially tailored optics and instrumentation could permit this technique to be applied at longer wavelengths, for example in the Er gain band, although longer wavelengths will necessarily compromise the spatial resolution. The total available optical path length shift constrained the spectral resolution of these measurements to be about 10 nm at 480 nm and about 40 nm at 1000 nm. Increasing the total applied phase shift would improve the spectral resolution and might permit the detection of interesting material dispersion characteristics in the vicinity of rare-earth absorption/emission bands. Increasing the effective dynamic range of the CCD detector beyond 8 bits would permit more accurate measurements in the vicinity of the short- and long-wavelength limits [15]. Only the phase components from the Fourier transforms were used here, but the Fourier amplitudes might be also used to measure absorption coefficients of rare-earth doped fibers in a spatially resolved fashion. The excellent spatial resolution of this technique could permit improved characterization of optical fiber gratings. This technique could also be applied to non-silica fibers (for example chalcogenide, phosphate, fluoride, bismuth, or polymer) by using appropriate index-matching fluids. Finally, instead of measuring an optical fiber, this technique could simultaneously measure the spectral and spatial distribution of refractive index of a fluid flowing through a capillary tube or cuvette [25].

V. Conclusion

In summary a technique for simultaneous measurement of

the refractive index of an optical fiber across more than one octave of bandwidth has been described. This data can be used to measure the material dispersion of the material comprising the optical fiber in a spatially resolved manner. Furthermore, since the refractive index measurement is made through the side of the optical fiber it can characterize refractive index changes along the length of the fiber, for example at a fusion splice or grating. This method achieves sub-µm spatial resolution and requires no assumptions about the symmetry or geometry of the optical fiber. Finally, the technique is applicable to silica glass, non-silica glass, or plastic optical fibers.

REFERENCES

[1] D. Marcuse, *Principles of Optical Fiber Measurement.* New York: Academic Press, 1981, ch. 4.

[2] N. M. Dragomir, G. W. Baxter, and A. Roberts, "Phase-sensitive imaging techniques applied to optical fibre characterisation," *IEE Proceedings – Optoelectronics*, vol. 153, pp. 217-221, 2006.

[3] F. El-Diasty, "Characterization of optical fibres by two- and multiple-beam interferometry," *Opt. Lasers in Eng.*.vol. 46, pp. 291-305, 2008.

[4] M. Sochacka, "Optical Fibers Profiling by Phase-Stepping Transverse Interferometry," *IEEE J. Lightwave Technol*., vol. 12, pp. 19-23, 1994.

[5] A.D. Yablon, *Optical Fiber Fusion Splicing*. New York: Springer, 2005, ch. 7.

[6] B. Bachim, and T. K. Gaylord, "Microinterferometric optical phase tomography for measuring small, asymmetric refractive-index differences in the profiles of optical fibers and fiber devices," *Appl. Opt.,* vol. 44, pp. 316-327, 2005.

[7] B. L. Bachim, T. K. Gaylord, and S. C. Mettler, "Refractive-index profiling of azimuthally asymmetric optical fibers by microinterferometric optical phase tomography," *Opt. Lett.*, vol. 30, pp. 1126-1128, 2005.

[8] B. Kouskousis, D. J. Kitcher, S. Collins, A. Roberts, and G. W. Baxter, "Quantitative phase and refractive index analysis of optical fibers using differential interference contrast microscopy," *Appl. Opt.*, vol. 47, pp. 5182-5189, 2008.

[9] H. M. Presby and I. P. Kaminow, "Binary silica optical fibers: refractive index and profile dispersion measurements," *Appl Opt.*, vol. 15, pp. 3029-3036, 1976.

[10] M. J. Adams, *An Introduction to Optical Waveguide*. New York: Wiley, 1981, pp. 244-245.

[11] J. W. Fleming, "Dispersion in GeO_2-SiO_2 glasses," *Appl. Opt.*, vol. 23, pp. 4486-4493, 1984.

[12] T. Kimura, in *Optical Fiber Transmission*, ed. by K. Noda, North Holland, 1986.

[13] O. V. Butov, K. M. Golant, A. L. Tomashuk, M. J. N. van Stralen, A. H. E. Breuls, "Refractive index dispersion of doped silica for fiber optics," *Opt. Communications,* vol. 213, pp. 301-308 (2002).

[14] T. J. Parker, "Dispersive Fourier transform spectroscopy," *Contemp. Physics*, vol. 31, pp. 335-353, 1990.

[15] V. Saptari, *Fourier-Transform Spectroscopy Instrumentation Engineering*. Bellingham, WA: SPIE press, 2003, ch. 1.

[16] E. C. T. Chao, "The application of quantitative interference microscopy to mineralogic and petrologic investigations," *American Mineralogist*, vol. 61, pp. 212-228, 1976.

[17] M. Pluta, *Advanced Light Microscopy Vol. 3: Measuring Techniques*. Amsterdam: Elsevier, 1993, ch. 16.

[18] N. Warnasooriya and M. K. Kim, "LED-based multi-wavelength phase imaging interference microscopy," *Opt. Express*, vol. 15, pp. 9239-9247, 2007.

[19] J. Schwider, "Advanced Evaluation Techniques in Interferometry," in *Progress in Optics XXVIII*, E. Wolf ed. Amsterdam: Elsevier, 1990, pp. 272-359.

[20] H. Schreiber and J. H. Bruning, "Phase Shifting Interferometry," in *Optical Shop Testing*, 3rd ed., D. Malacara ed. New York: Wiley, 2007, pp. 547-666.

[21] Igor Pro ver. 6.10Beta, Wavemetrics, P.O. Box 2088 , Lake Oswego, OR, 97035, www.wavemetrics.com.

[22] P.L. Chu and T. Whitbread, "Nondestructive determination of refractive index profile of an optical fiber: fast Fourier transform method," *Appl. Opt.*, vol. 18, pp. 1117-1122, 1979.

[23] M. R. Hutsel, C. C. Montarou, A. I. Dachevski, and T. K. Gaylord, "Algorithm performance in the determination of the refractive-index profile of optical fibers," *Appl. Opt.*, vol. 47, pp. 760-767, 2008.

[24] National Physics Laboratory, Middlesex, UK, see "http://www.npl.co.uk/optical-radiation-photonics/optical-comms-and-data/products-and-services/optical-fibre-refractive-index"

[25] A. Yang, W. Li, G. Yuan, J. Dong, J. Zhang, "Measuring the refractive indices of liquids with a capillary tube interferometer," *Appl. Opt.*, vol. 45, pp. 7993-7998, 2006.

[26] A. D. Yablon, "Multi-Wavelength Optical Fiber Refractive Index Profiling by Spatially Resolved Fourier Transform Spectroscopy," presented at OFC/NFOEC, San Diego, CA, March 22-26, 2009, Postdeadline Paper PDP A2.

Andrew D. Yablon (M'97) was born in New York City in 1970. He earned the S.B. degree in 1992, the S.M degree in 1993, and the Ph.D. degree in 1997, all in mechanical engineering, and all from M.I.T. in Cambridge, MA, USA.

From 1998 until 2000 he was Senior Research Scientist at Vytran Corporation in Morganville, NJ, where he developed novel fiber processing and fusion splicing technologies. From 2000 until 2008 he was a Member of Technical Staff at Bell Laboratories in Murray Hill and later OFS Laboratories in Somerset, NJ. Currently he serves as President of Interfiber Analysis in Livingston, NJ, USA, which he founded in 2008. He has participated as an author on over 50 peer reviewed publications, holds 12 US Patents, and recently wrote the textbook Optical Fiber Fusion Splicing (New York, NY: Springer, 2005). His current research interests include optical fiber refractive index measurement, optical fiber interconnection, fusion splicing, and fiber mechanical properties.

Dr. Yablon is a member of SPIE, OSA and IEEE. He is the chair for the OFC/NFOEC 2010 Subcommittee A: Fibers and Optical Propagation Effects and teaches a course entitled "Interconnection and Splicing of High-Power Optical Fibers" at SPIE Photonics West.